Multiple-scattering approaches to carbon K-shell near-edge X-ray absorption fine structure of graphite

1994 J. Phys.: Condens. Matter 6 2949

(http://iopscience.iop.org/0953-8984/6/15/017)

J. Phys.: Condens. Matter 6 (1994) 2949–2956. Printed in the UK

Multiple-scattering approaches to carbon K-shell near-edge x-ray absorption fine structure of graphite

Y Zou and J C Tang

Physics Department, Zhejiang University, 310027 Hangzhou, People's Republic of China

Received 6 October 1993, in final form 16 December 1993

Abstract. The multiple-scattering cluster method was first employed to calculate the theoretical near-edge x-ray absorption fine structure (NEXAFS) spectrum of graphite. Studies on the polarization dependence on the incident vector E classify spectral features into π and σ resonances. Characterization of the carbon K-shell NEXAFS spectra of the species modelled by both a single layer and a multilayer has been performed. It reveals that a π^* resonance originally located at around 289 eV splits with the accumulation of the number of atoms included in the cluster. Multilayer calculation has little influence on the NEXAFS spectrum. Our calculation coincides with the experimental results fairly well. In addition, it has been found to be in good agreement with the final density of states derived from band-structure calculations.

1. Introduction

The near-edge x-ray absorption fine structure (NEXAFS) technique shows great promise as a site-specific probe of electronic and geometric structure. It plays an important role not only in the microscopic characteristics of surface chemisorption [1, 2] but also in the structural determination of the intramolecular bond length of gaseous molecules [3] or the configuration of amorphous films [4]. Carbon is of particular interest because of the extensive distribution on Earth and the fact that it is an essential part of all lifeforms. However, x-ray fine-structure measurements have been confined to above 3000 eV owing to the experimental difficulties encountered at lower photon energies [5]. It was not until 1980 that monochromatic radiation of sufficient resolution and intensity above the carbon K edge (285 eV) was available. Since then, great efforts have been made in the structural studies of linear hydrocarbons [6], gaseous and condensed cyclic hydrocarbons [7], aromatic molecules [8] and amorphous carbon films [4]. Crystalline carbon in the form of graphite is one of the most comprehensively studied materials both experimentally and theoretically. Because of its layered structure with a relatively large separation between layers, graphite is often modelled as a two-dimensional solid. In addition, knowledge of the properties of graphite is a starting point for understanding intercalated graphite, which is a field of very active research [9].

Studies of the graphite carbon K-edge NEXAFS spectrum have been performed on non-single-crystal samples [10] as well as on crystalline graphite [11]. There have been several calculations of the band structure of graphite [12, 13]. The calculated conduction band can be related to unoccupied antibonding states [14], which are shown as characteristics in the NEXAFS spectrum. Furthermore, the experimental NEXAFS spectra of graphite demonstrate that the excitation to the final states σ^* or π^* depends on the polarization direction of the incident x-ray [15]. It is well known that multiple scattering appears prominently in the

0953-8984/94/152949+08$19.50

energy range no more than 50 eV above the K edge. There should be a suitable method for dealing with such a complicated situation aimed at extracting potential structural information from experimental data. This is just what has been done for the much higher-energy-range EXAFS analysis.

In this paper, we present multiple-scattering cluster (MSC) method [16] theoretical studies of the carbon K-edge NEXAFS of graphite. This method has been extremely helpful in surface chemisorption studies [17, 18]. Here we firstly apply the MSC method to solid bulk materials such as graphite. Looking upon the six-member ring as a structural unit, we construct several clusters with various numbers of honeycombs. When the number of honeycombs increases, the calculated result undergoes an evolution from a spectrum resembling that of benzene to a spectrum analogous to that of graphite, in which we find π^* resonance splitting due to the two-dimensional magnitude increase. Three layers are chosen to simulate the graphite multilayer structure. The calculated results, compared with that of single layer, show that the interlayer has little effect except for a slight difference at the higher-energy position.

2. Description of the MSC method of NEXAFS

The dynamic theory of photoelectron diffraction (PD) has been developed by some workers [19–21]. In their Green function formalism the multiple-scattering effect was considered in terms of the t-matrix method. The similarity between NEXAFS and photoemission encourages us to describe the wavefunction of an intermediate photoelectron in NEXAFS by that in PD. The detailed derivation of formalism can be seen elsewhere [17].

In our MSC method, we have considered all multiple-scattering effects in a cluster simulating the species studied, which consists of one central absorbing atom and several neighbouring atoms. Our NEXAFS study shows that this approximation is correct. It has been demonstrated that the atoms near an adsorbing centre contribute most to the NEXAFS spectrum because photoelectrons excited by near-edge x-ray radiation are limited to having a low kinetic energy. Usually we choose 20 or fewer atoms to construct the cluster for NEXAFS studies. Our computer capacity enables us to add no more than 70 atoms to the cluster so as to calculate very complex molecules or structures. The summation of all scattering events is taken over all the individual atoms rather than over the atomic shells [22]. The inputs to the calculation of NEXAFS spectra in terms of the MSC method include the positions of the atoms in the cluster, the incident photon direction and the phase shift δ_l, which are calculated by the muffin-tin potential in the cluster. We superimpose the self-consistent X_α atomic charge densities to obtain this cluster potential. It is found that the phase shifts mentioned above are in good agreement with those calculated by the SCF X_α SW method.

3. Results and discussion

3.1. Analysis of the NEXAFS spectrum of the C_6 ring

We start our studies with the simple-structure honeycomb, i.e. the six-member ring. The C_6 ring is a structural unit in graphite and resembles benzene and other cyclic hydrocarbon compounds. The carbon K-shell NEXAFS spectra of benzene in the gas phase, solid state and chemisorbed states have been measured by Horsley *et al* [23]. We have plotted their experimental spectrum of solid benzene in figure 1, curve (I). According to [23], peaks 1 and 2 are both assigned π^* resonances, and the other two peaks 3 and 4 are attributed to σ^*

shape resonances. The assignment was experimentally examined in terms of polarization dependence, but there exist a number of conflicting assignments [6, 24] for the benzene spectrum. In order to obtain a better understanding of π^* and σ^* resonances in complex molecules, we think that an easy way would be to determine the carbon K-edge NEXAFS spectrum of the C_6 ring by the MSC method.

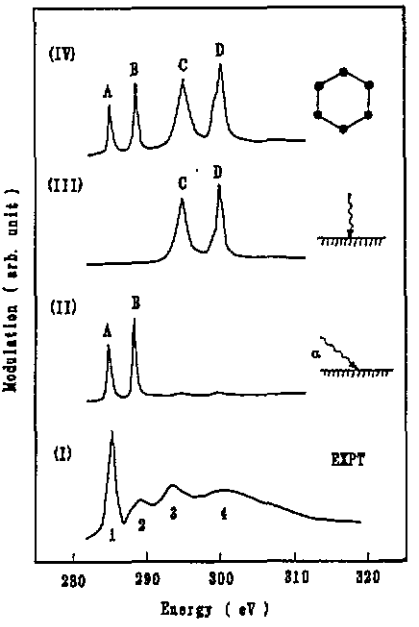

Figure 1. Characterizations for the carbon K-edge NEXAFS spectrum of benzene C_6H_6 compared with calculations of the six-member ring (the six-member ring is shown at the top inset as a honeycomb); curve (I), experimental spectrum of solid benzene [23]; curve (II), calculated spectrum for glancing incidence angle with $\alpha = 10$; curve (III), calculated perpendicular-incidence spectrum, with the vector E parallel to the ring plane; curve (IV), unpolarized spectrum of the honeycomb structure.

We choose the C–C bond length to be 1.4210 Å, a commonly accepted bond length value for graphite, and the C–C–C bond angle θ to be 120°. The cluster is shown in the top inset of figure 1. We plotted the calculated NEXAFS spectra as curves (II)–(IV) in this figure. Three curves are considered for different incidence conditions. Curve (IV) is the spectrum with unpolarized x-rays. Four peaks A, B, C, and D can be clearly seen in this curve; these agree fairly well with the experimental peak positions whereas their absolute peak intensities are not reproduced. The widths of peaks A and B are relatively much narrower than those of peaks C and D, which suggests that the latter correspond to continuum shape resonance. All the main features in the spectrum for benzene have been accurately reproduced, and some weak features between peak 1 and peak 2 exist in the experimental spectrum which have been ascribed to a mixture of Rydberg state and C–H resonance [7]. In contrast, such features are not presented in our calculation owing to the absence of hydrogen atoms in cluster models. Furthermore, we have performed two polarization calculations. For curve (II), the vector E is closely perpendicular to the ring plane at a glancing incidence angle at 10°. As expected, resonances A and B are excited intensely while peaks C and D are very weak. In contrast with curve (II), peaks C and D on

curve (III) have predominant intensities while peaks A and B disappear. From polarization considerations [15], we unambiguously draw the conclusion that peaks A and B are π^* resonances, and peaks C and D are σ^* resonances.

3.2. The π^* splitting of the graphite single-layer model

We increase the number of honeycombs in the single-layer basal plane in graphite. Our purpose is to observe what will happen accompanied by the structural change from a simple C_6 ring to graphite. In order to evaluate this change, we have calculated the spectra corresponding to five different clusters which include six, 13, 22, 37 and 52 atoms, respectively. The latter four clusters are shown in figure 2. All the calculations are polarization independent. The results have been plotted in figure 3, curves (I)–(V). In these calculations the values of the bond length and the bond angle are the same as those in the C_6 ring. The experimental spectrum with the polarization angle $\alpha = 50°$ investigated by Rosenberg *et al* [15] is also plotted in the same figure.

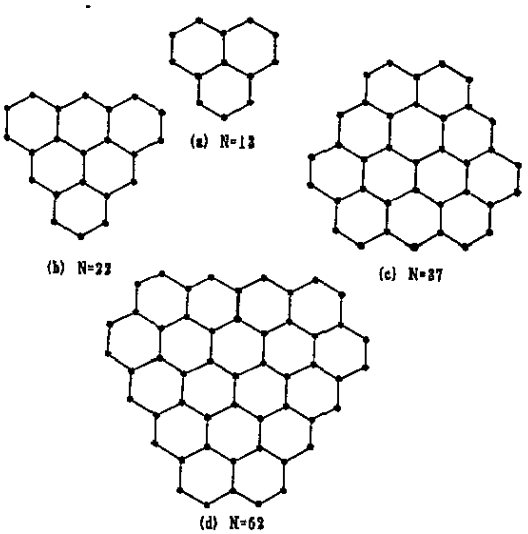

Figure 2. Different single-layer cluster models involved in the calculation for the carbon K-edge NEXAFS of graphite. The number N of atoms in the cluster varies from 13 to 52.

With respect to the 13-atom cluster, peak A in curve (I) for the C_6 ring shifts to a higher energy and is labelled in curve (II) as A′, then it splits into two new π^* resonances labelled B and C in curve (III) for the 22-atom cluster. Peak C is much closer to the σ^* continuum shape resonance. More π^* resonances appear for the larger cluster with $N = 37$. Besides the splitting in the previous region, there arises a new resonance G which is below the original π^* resonance 1. Peak F overlaps the σ^* resonance. The addition of an extra 15 atoms to the 37-atom cluster creates a rather huge cluster with $N = 52$. The fact that its spectrum resembles that of the cluster with $N = 37$ indicates the convergence of the calculation. A polarization study reveals that π^* and σ^* resonances degenerate around peak 2′, while the σ^* resonance makes a higher contribution to the formation of peak 2′ than the π^* resonance does. All the σ^* resonances 2′–5′ on curve (V) are in good agreement with the experimental features 2–5 when all the other polarization situations in [15] are taken into account.

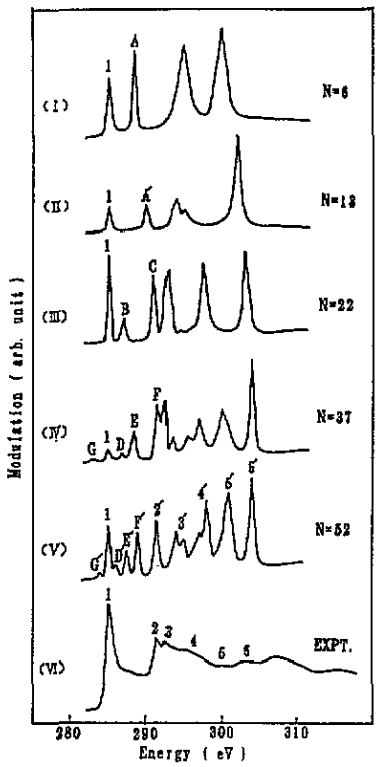

Figure 3. Analysis of π^* resonance splitting in the spectra for the graphite carbon K-edge NEXAFS: curves (I)–(V), calculated spectra for different models with N from 6 to 52; curve (V), σ^* resonances labelled 2′–5′ in comparison with the experimental features 2–5; curve (VI) experimental spectrum of HOPG [15]. In our calculated results, π^* resonances are especially labelled. The peak with a fixed energy position in all curves at around 285 eV was labelled 1. N is the number of atoms in different single-layer clusters.

From the experimental graphite spectrum, only one obvious π^* resonance can be observed at around 285 eV. However, it has been noted [11, 15] that a kink occurs at an energy of around 286.6 eV, which just falls into our predicted splitting region. However, no more weak structures exist between 285 and about 290 eV in the experimental data. A calculation of the π-band density of states [13] has revealed that a maximum occurs at around 285 eV whereas the density of states decreases rapidly below and above this energy. Therefore the π^* resonance at 285 eV is significantly enhanced while other resonances are suppressed because of the final-state effect. This can explain why only one π^* resonance appears in the graphite spectrum, and the appearance of the kink can be ascribed to the incomplete suppression. The intensity variation in peak 1 deserves further detailed discussion. While the number of atoms included in the cluster varies from $N = 6$ to $N = 52$, its intensity experiences an increase or a decrease with respect to the most intensive σ^* resonance. An additional shell added to a cluster with fewer atoms can unambiguously either strengthen or weaken the peak intensity. This is a subtle effect caused by multiple scattering between different shells. Another interesting point is the accurate Fermi level in graphite. It has been reported that, for stage-1 $FeCl_3$-intercalated graphite, a peak is observed at 285 eV, accompanied by new structure between 283.2 and 284.2 eV [11],

which demonstrates a lowering of the Fermi level from the threshold 284.7 eV value to about 283 eV and has been ascribed to intercalation. From our theoretical study, we find that peak G increases at around 283.5 eV. Thus the Fermi level of graphite should be about 283 eV. The intercalation really does make a contribution to the Fermi level position, but also it changes the original π-band density-of-states distribution, especially around the Fermi level, owing to charge transfer between the intercalant and graphite. As a result, the π^* resonance suppressed before intercalation becomes an observable structure in the NEXAFS spectrum.

3.3. Interlayer interaction studies in graphite

To study the interlayer effect in graphite, we selected three layers of graphite to construct the two different clusters shown in figure 4. The layer spacing was taken to be 3.359 Å. Two clusters have the same number of atoms as their corresponding single layer. Owing to limited computer capacity, we have to choose fewer atoms in the middle layer; so the spectrum produced cannot coincide well with the experimental results. As we shall pay more attention to the interlayer effect, this does not seem to pose a serious problem. Our calculations are shown in figure 5. Curves (V) and (IV) for the clusters with $N = 13$ and $N = 21$, respectively, are almost the same, except for an insignificant feature for the $N = 21$ cluster at around 310 eV. Curves (II) and (III) are also nearly the same, apart from a feature located at 295 eV which has been intensified compared with single-layer model and also a feature at around 310 eV which does not occur for the single layer. In fact the introduction of extra layers does cause a slight difference but there is no considerable change from the features for a single layer. In the graphite layer, carbon atoms are bonded together with sp^2 hybridized orbitals while the interaction between layers arises from the van der Waals force. The former affects the multiple-scattering process much more strongly than does the latter. Therefore, we conclude that multilayer interaction plays a less significant role in the near-edge structure of the graphite-like film.

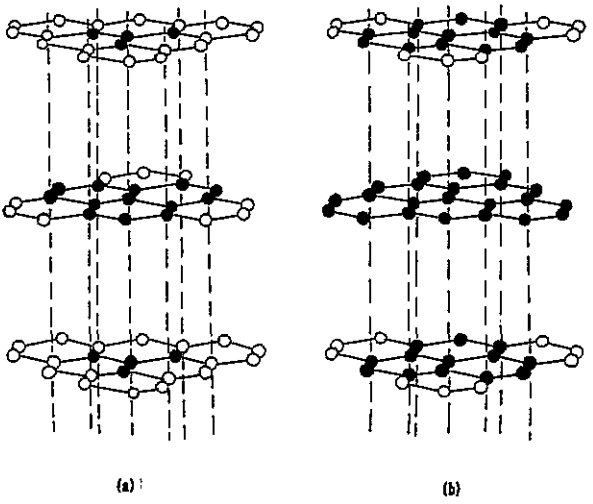

Figure 4. Clusters modelled as three layers in graphite. The atoms involved in the cluster are shown as full circles. (*a*) The middle layer has 13 atoms; the other two layers both have four atoms. (*b*) The middle layer has 22 atoms; the other two layers both have 19 atoms.

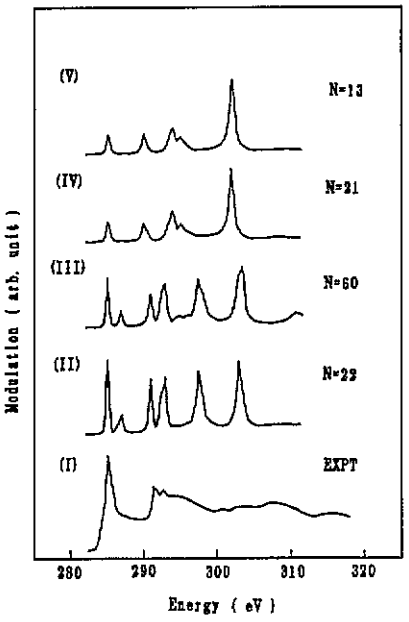

Figure 5. Studies of the interlayer interaction between the layers in graphite. In curves (III) and (IV), the middle layer has the same number of atoms as their corresponding single-layer models (II) and (V), respectively.

4. Conclusion

We have calculated the carbon K-shell NEXAFS for graphite. The six-member ring plays a unique role in our studies. With its help, we can assign two π^* resonances in benzene. As the cluster that consists of several honeycombs gradually approaches the graphite layer structure, π^* splitting becomes more obvious. Because of the density-of-states distribution, only a π^* resonance at 285 eV appears while other π^* resonances disappear. We determine the accurate Fermi level, which illustrates that the intercalant contributes to the rearrangement of the π density of states near Fermi level. A three-layer model calculation reveals that little interlayer interaction is involved in the NEXAFS spectrum of graphite.

Acknowledgments

The authors are pleased to acknowledge the support of the National Natural Science Foundation of China and the Zhejiang Province Natural Science Foundation.

References

[1] Tourillon G, Mahatsekake C, Andrieu C, Williams G P, Garrett R F and Braun W 1988 *Surf. Sci.* **201** 171
[2] Hoffmann H, Zaera F, Ormerod R M, Lambert R M, Wang L P and Tysoe W T 1990 *Surf. Sci.* **232** 259
[3] Sette F, Stöhr J and Hitchcock A P 1984 *J. Chem. Phys.* **81** 4906
[4] Comelli G, Stöhr J, Robinson C J and Jark W 1988 *Phys. Rev.* B **38** 7511
[5] Stöhr J, Jaeger R, Feldhaus J, Brennan S, Norman D and Apai G 1980 *Appl. Opt.* **19** 3911
[6] Hitchcock A P and Brion C E 1977 *J. Electron Spectrosc.* **10** 317

[7] Hitchcock A P, Newbury D C, Ishii I, Stöhr J, Horsley J A, Redwing R D, Johnson A L and Sette F 1986 *J. Chem. Phys.* **85** 4849
[8] Johnson A L, Mutterties E L and Stöhr J 1983 *J. Am. Chem. Soc.* **105** 7183
[9] Fischer J E and Thompson T E 1980 *Phys. Today* **31** 36
[10] Denley D, Perfetti P, Williams R S and Shirley D A 1980 *Phys. Rev.* B **21** 2267
[11] Mele E J and Ritsko J 1979 *Phys. Rev. Lett.* **43** 68
[12] Willis R F, Fitton B and Painter G S 1974 *Phys. Rev.* B **9** 1926
[13] Tatar R C and Rabii S 1982 *Phys. Rev.* B **25** 4126
[14] Sette F, Stöhr J and Hitchcock A P 1984 *Chem. Phys. Lett.* **110** 519
[15] Rosenberg R A, Love P J and Rehn V 1986 *Phys. Rev.* B **33** 4034
[16] Tang J C, Fu S B, Ji H and Chen Y B 1992 *Sci. China* A **35** 965
[17] Tang J C, Feng X S, Shen J F, Fujikawa T and Okazawa T 1991 *Phys. Rev.* B **44** 13018
[18] Tang J C and Feng X S 1992 *Japan. J. Appl. Phys.* **32** Suppl. 374
[19] Liebsch A 1976 *Phys. Rev.* B **13** 544; 1977 *Phys. Rev. Lett.* **38** 248
[20] Li C H, Lubinsky A R and Tong S Y 1978 *Phys. Rev.* B **17** 3128
[21] Lindsay R N and Pendry J B 1978 *J. Phys. C: Solid State Phys.* **11** 1031
[22] Durham P J, Pendry J B and Hodges C H 1982 *Comput. Phys. Commun.* **25** 193
[23] Horsley J A, Stöhr J, Hitchcock A P, Newbury D C, Johnson A L and Sette F 1985 *J. Chem. Phys.* **83** 6099
[24] Butscher W, Schwarz W H E and Thunemann K H 1981 *Inner Shell and X-ray Physics of Atoms and Solids* ed D J Fabian, H Kleinpoppen and L Watson (New York: Plenum)